ELSEVIER

Chemical Engineering Journal 134 (2007) 209–217

Chemical Engineering Journal

www.elsevier.com/locate/cej

A two dimensional steady-state model of the gas–solid–solid reactor Example of the partial oxidation of methane to methanol

Carlos Gregorio Dallos [a,*], Viatcheslav Kafarov [a], Rubens Maciel Filho [b]

[a] *Chemical Engineering Department, Industrial University of Santander, Bucaramanga, AA 678 Bucaramanga, Colombia*
[b] *Chemical Engineering Department, State University of Campinas, Campinas, SP, Brasil*

Abstract

This work presents the modeling and the selection of best topology of gas–solid–solid reactor for direct synthesis of methanol from methane. A gas–solid–solid system is used for such a purpose consisting of a catalyst fixed bed and a second solid that flow in counter-current with the flowing gas. A selective adsorption system enables the intensification of the partial oxidation of methane increasing more than 12 times the methanol production. The solution of the mass, energy and momentum transfer equations for a gas–solid–solid catalytic system was developed with Fortran and the NAG mathematical libraries.

Keywords: Methane; Methanol; Gas–solid–solid reactor

1. Introduction

1.1. Partial oxidation of methanol

Methanol production is a very importance industry due to its high consumption as chemical precursor. The industrial process uses methanol as feedstock, which is catalytically transformed first in synthesis gas and later in methanol. This process implies the handling of high level of recycle and therefore high-energy consumptions.

Partial oxidation of methane is an explored alternative for the production of the methanol. The search is focus in the synthesis of new catalysts and search of optimal conditions of reaction for both: homogeneous and heterogeneous reaction [1–33]. Catalysts of iron phosphate, molybdenum, vanadium, copper and zinc among other have been developed with relative success and some authors show very complete kinetic studies that offer information of the reaction parameters and their variation with the temperature.

Most of the studies of partial oxidation show competitive reactions, mainly the acetaldehyde and carbon oxides formation, which in many of the cases, have a bigger selectivity that the methanol formation. In most of the cases the operational conditions to which the selectivity to methanol is favored the reaction rate is very low. This problem means that this route is not applicable at industrial level at the moment.

1.2. Gas–solid–solid reactor

A gas–solid–solid (GSS) contactor is a special type of reactor that consists of a packed bed with solids (generally a catalyst) and a second solid that can flow in co-current or counter-current with the flowing gas. This kind of reactor has been proposed for applications of heat exchange, catalysts regeneration, gases purification and low conversion reactions intensification among others. An interesting work was presented by Westerterpt and collaborators [34–36], in which showed a mathematical model and the prototype of a small-scale gas–solid–solid reactor for the intensification of the methanol formation using synthesis gas as feedstock. Yields were achieved of more than 80% in a single step.

One of the aspects that have limited the use of gas–solid–solid contactors is the complexity associated with the interactions between the gas and the moving particles. Estimation of the velocity and the residence time of the solids in movement, and the gas pressure drop through the bed have been the target of multiple studies that tried to find a flow model for this GSS reactor [37–41]. Gases and particles movement analysis in a GSS reactor can also be developed by techniques of computational fluid dynamics (CFD). This approach implies the direct use of continuity and momentum equations. For the solution of the CFD

---

[*] Corresponding author. Tel.: +57 7 6344746; fax: +57 7 6344684.
E-mail address: cisyc@uis.edu.co (C.G. Dallos).

1385-8947/$ – see front matter © 2007 Elsevier B.V. All rights reserved.
doi:10.1016/j.cej.2007.03.044

Nomenclature

a, b	state equation parameters
b	affinity constant of the adsorbent
B_i, F_c, G_i, y	auxiliary functions
C	adsorbed species concentration
C_H	adsorbent saturation constant
D	diffusion coefficient
$\vec{g}$	gravitational acceleration
k	reaction rate
k	Boltzmann constant
k_D	Henry dissolution constant
M	molecular weight
$\bar{q}$	conductive heat flux
$\bar{\bar{q}}_\theta$	diffusive granular energy flux
$\bar{\bar{S}}$	stress tensor
T	temperature
T^*	dimensionless temperature
$\vec{v}$	velocity
V	molar volume
X	molar fraction

Greeks letters

ε	volumetric fraction
γ	energy transfer coefficient
γ_{θ_s}	granular energy dissipation due to inelastic collisions
η	viscosity coefficient
η^*	auxiliary function
λ	thermal conductivity
Θ	granular temperature
$\sum v$	volumes for fuller diffusions
ρ	density
$\bar{\bar{\tau}}$	elastic stress tensor
ω	acentric factor

Subscripts

c	critical point property
g	gas phase property
i	chemical specie property
j	chemical reaction parameter
m	mixture property
r	reduced property
s	solid phase property

partial differential equations the used of specialized programs developed in the last decade is of great use.

The aim of this paper was the development of a model for a new type of reactor applied to the partial oxidation of methane to methanol. This reactor consisted of a GSS contactor that can increase the chemical reaction conversion by using an adsorbent that selectively removes the product from the reaction area, as schematically shown in Fig. 1. This modeling methodology allowed us to design the best topology for the reactor system applied to the direct synthesis of methanol from methane.

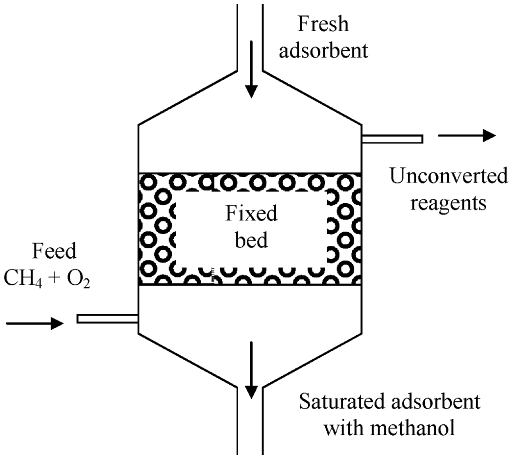

Fig. 1. Basic scheme of a gas solid–solid reactor for partial oxidation of methane to methanol.

2. Methodology

2.1. Selective adsorbent selection

The first part of this study is the search for a selective adsorbent that allows removing the methanol from the reaction area. To determine the model parameters for adsorption on the selected samples we used the methodology for identification of parameters in catalysts and adsorbents developed in the project "New method for the investigation of catalysts and adsorbents". This used procedure has been broadly described in previous works [42–44].

Tests were carried out with different commercial adsorbents of silica, silica–alumina, and well-known adsorbents, such as activated coal and alumina. These tests were made in the temperature range of 150–260 °C. Preliminary tests at temperatures higher than 260 °C showed that methanol adsorption was reduced in all the used adsorbents. The obtained results showed that the material that presents the best characteristics of methanol adsorption in comparison with formaldehyde adsorption was the silica–alumina adsorbent.

2.2. Kinetic model

In this work, chemical reactions in two phases were taking into account: homogeneous chemical reaction in the gas phase and catalytic chemical reaction to the interior of a solid catalyst.

2.3. Homogeneous chemical reaction

To guarantee the trust in the results of the mathematical model, it is convenient, as a first and logical step towards the rational and complete description of the overall system, to verify the possibility of simulating and predicting the behavior of the homogeneous system. Though the detailed homogeneous part of the methane oxidation involves more than 1000 elementary reaction steps and 60 reacting species [21].

An important amount of theoretical and experimental studies has been developed in recent years by different authors to

Table 1
Parameters for the rate of reactions in homogeneous gas phase

Chemical reaction	Forward rate			Backward rate		
	A (mol, cm^3, s, K)	*n*	*E* (cal/mol)	A (mol, cm^3, s, K)	*n*	*E* (cal/mol)
$CH_3OH \Leftrightarrow OH + CH_3$	3.02E+18	0	80,000	1.78E+11	0	−10,985
$O_2 + CH_3OH \Leftrightarrow HO_2 + CH_2OH$	3.98E+10	0	50,910	1.46E+04	0	37,972
$H + CH_3OH \Leftrightarrow CH_3 + H_2O$	5.25E+12	0	5,340	2.07E+12	0	36,950
$H + CH_3OH \Leftrightarrow CH_2OH + H_2$	3.02E+13	0	7,000	3.24E+07	0	51,770
$OH + CH_3OH \Leftrightarrow CH_2OH + H_2O$	3.98E+12	0	2,000	1.85E+07	0	61,925
$O + CH_3OH \Leftrightarrow OH + CH_2OH$	1.70E+12	0	2,290	7.99E+05	0	44,965
$CH_3 + CH_3OH \Leftrightarrow CH_2OH + CH4$	1.82E+11	0	9,800	5.09E+05	0	55,050
$HO_2 + CH_3OH \Leftrightarrow H_2O_2 + CH_2OH$	6.31E+12	0	19,360	9.23E+06	0	48,058
$CH_2OH \Leftrightarrow H + CH_2O$	2.51E+13	0	29,000	4.14E+13	0	−35,030
$CH_2OH + O_2 \Leftrightarrow HO_2 + CH_2O$	1.00E+12	0	6,000	8.74E+17	0	−8,298
$H + CH_2OH \Leftrightarrow CH_2O + H_2$	3.01E+12	0	0	7.69E+18	0	43,410
$CH_4 \Leftrightarrow H + CH_3$	2.00E+17	0	88,000	4.94E+10	0	−19,920
$O_2 + CH_4 \Leftrightarrow CH_3 + HO_2$	7.94E+13	0	56,000	1.04E+13	0	−2,188
$H + CH_4 \Leftrightarrow CH_3 + H_2$	2.24E+04	3	8,750	8.57E+03	3	8,270
$OH + CH_4 \Leftrightarrow CH_3 + H_2O$	3.47E+03	3.08	2,000	5.75E+03	3.08	16,675
$O + CH_4 \Leftrightarrow OH + CH_3$	1.18E+07	2.08	7,630	1.98E+06	2.08	5,055
$HO_2 + CH_4 \Leftrightarrow CH_3 + H_2O_2$	2.00E+13	0	18,000	1.04E+13	0	1,448
$OH + CH_2O \Leftrightarrow HCO + H_2O$	7.59E+12	0	170	2.62E+12	0	29,997
$H + CH_2O \Leftrightarrow HCO + H_2$	3.31E+14	0	10,500	2.64E+13	0	25,172
$O + CH_2O \Leftrightarrow OH + HCO$	5.01E+13	0	4,600	1.76E+12	0	17,177
$HO_2 + CH_2O \Leftrightarrow HCO + H_2O_2$	1.00E+12	0	8,000	1.09E+11	0	6,600
$HCO \Leftrightarrow H + CO$	1.45E+14	0	19,000	6.12E+08	0	1,558
$HCO + O_2 \Leftrightarrow HO_2 + CO$	3.31E+12	0	7,000	7.43E+12	0	39,290
$OH + HCO \Leftrightarrow CO + H_2O$	1.00E+14	0	0	2.84E+15	0	105,133
$H + HCO \Leftrightarrow CO + H_2$	2.00E+14	0	0	1.31E+15	0	89,998
$O + HCO \Leftrightarrow OH + CO$	1.00E+14	0	0	2.88E+14	0	87,903
$O + CO \Leftrightarrow CO_2$	5.89E+15	0	4,100	4.48E+23	0	131,780
$CO + O_2 \Leftrightarrow O + CO_2$	2.51E+12	0	47,690	2.22E+13	0	53,910
$OH + CO \Leftrightarrow H + CO_2$	1.51E+08	1.3	−770	1.70E+10	1.3	21,565
$HO_2 + CO \Leftrightarrow OH + CO_2$	5.75E+13	0	22,930	6.53E+14	0	84,763
$H_2 + O_2 \Leftrightarrow OH + OH$	1.70E+13	0	47,780	5.90E+11	0	29,570
$OH + H_2 \Leftrightarrow H + H_2O$	1.17E+09	1.3	3,626	5.07E+09	1.3	18,781
$O + OH \Leftrightarrow H + O_2$	4.00E+14	−0.5	0	5.07E+15	−0.5	16,115
$O + H_2 \Leftrightarrow H + OH$	5.06E+04	2.67	6,290	2.22E+04	2.67	4,195
$H + O_2 \Leftrightarrow HO_2$	3.61E+17	−0.72	0	1.91E+23	−0.72	49,732
$OH + HO_2 \Leftrightarrow O_2 + H_2O$	7.50E+12	0	0	9.49E+13	0	72,863
$H + HO_2 \Leftrightarrow {}_2*OH$	1.40E+14	0	1,073	1.42E+13	0	40,571
$O + HO_2 \Leftrightarrow OH + O_2$	1.40E+13	0	1,073	1.80E+13	0	56,685
$OH + OH \Leftrightarrow O + H_2O$	6.00E+08	1.3	0	5.92E+09	1.3	17,250
$H + H \Leftrightarrow H_2$	1.00E+18	−1	0	1.55E+24	−1	107,440
$H + OH \Leftrightarrow H_2O$	1.60E+22	2	0	1.07E+29	2	122,593
$O + O \Leftrightarrow O_2$	1.89E+13	0	−1,788	1.63E+21	0	119,672
$H + HO_2 \Leftrightarrow H_2 + O_2$	1.25E+13	0	0	3.65E+13	0	57,708
$HO_2 + HO_2 \Leftrightarrow H_2O_2 + O_2$	2.00E+12	0	0	7.98E+12	0	41,636
$H + H_2O_2 \Leftrightarrow HO_2 + H_2$	1.60E+12	0	3,800	1.17E+12	0	19,872
$OH + H_2O_2 \Leftrightarrow H + H_2O$	1.00E+13	0	1,800	5.99E+07	0	−16,705

establish a reliable model for the combustion and partial oxidation of methane in the gas phase: Westbrook and Dryer [10] formulated a chemical kinetic modeling of hydrocarbons combustion including methane; Strehlow [11] showed a fundamental study about hydrocarbon combustion; Pitz and Westbrook [12] made a chemical kinetics study of the high pressure oxidation of hydrocarbons; Dagaut et al. [13] formulated a kinetic modeling of hydrocarbon oxidation; Bartok and Sarofim [14] gathered kinetic studies in a very complete handbook about fossil combustion; Okazaki et al. [15] developed experimental studies of the direct conversion of methane to methanol; Bistol et al. [16] formulated a kinetic model for the methane oxidative coupling reactions; Rajnikanth et al. [17] studied the methanol synthesis in plasma discharges; Kodama et al. [18] studied the high-temperature reactions between CH_4, H_2O, C_2H_4, CO and H_2; Warnatz et al. [19] gathered kinetic studies of methanol and other hydrocarbon in their combustion handbook; Feitelberg and Corream [20] carried out a study about the reactions between CO, N_2 and nitrogen oxides under combustion conditions.

Based on the above-mentioned works, Verma [21] gathered a complete kinetic model for homogeneous gas phase reactions for the partial oxidation of methane to methanol, the rate constants for the involved reactions were selected from references [10–20]. The temperature level, i.e. from 35 to 700 °C, adopted for methane oxidation in Verma's work is also similar to temperatures generally used in the catalytic conversion of methane into methanol. Therefore, in the present work, we used Verma's model for homogeneous chemical reaction in the gas phase taking into account a set of 46 elementary reactions for 16 chemical species with their respective kinetic parameters (Table 1). The main methane oxidation path considered can be represented as:

$$CH_4 \Leftrightarrow CH_3 \Leftrightarrow CH_3OH \Leftrightarrow CH_2$$

$$OH \Leftrightarrow CH_2O \Leftrightarrow CHO \Leftrightarrow CO_2 + H_2O$$

The equation used to calculate the reaction rates is:

$$k_j = AT^n e^{-E/RT} \tag{1}$$

The contribution of the direct gas phase oxidation of methane into methanol must be coupled with a catalytic conversion on the solid to improve the common production of methanol.

2.4. *Catalytic chemical reaction*

Numerous theoretical and experimental studies have been developed in the search for successful catalysts for the catalytic partial oxidation of methane: Amiridis et al. [22] developed a simulation to describe the partial oxidation of methane over silica-supported molybdenum and vanadium and formulated a microkinetic reaction model; Paredes Olivera et al. [27] developed a theoretical work showing that the direct synthesis of methanol over noble metals may proceed mainly on less active metals, such as Pt and Au, while on Ni the model predicts that methane will be oxidized to CO and CO_2; Knops-Gerrits and Goddard [29] showed a theoretical and experimental study of the methane partial oxidation over iron zeolites; Takemoto et al. [30] studied the effects of reaction pressures on the oxidation of methane with O_2 and NO over a Cu-ZnO/Al_2O_3 catalyst. They found a maximum yield of CH_3OH at 0.4 MPa and a feed ratio CH_4/O_2 of 8.0; Zhang [31] investigated the partial oxidation to methanol and formaldehyde on a Mo-V-Cr-Bi-Si oxide catalyst in a tubular reactor between 380 and 530 °C; Wang et al. [32] showed an experimental study of the iron phosphate catalyst for partial oxidation of methane. They proposed models for the kinetic reaction rate with both oxygen and nitrous oxide. Amiridis et al. [22], Chellappa and Viswanath [23], and Chellappa [24] showed that the MoO_3-Fe_2O_3 catalyst is one of the best catalytic systems for the partial oxidation of methane. So, in the present work for the catalytic heterogeneous reaction, the ferric molybdate catalyst studied by Fuangfoo [33] was selected. The work by Fuangfoo shows the most complete set of kinetic parameters, and the mechanism formulated is in general agreement with the mechanism suggested in previous works by Amiridis et al. [22] based on kinetic studies, and the results of Spencer and Pereira [25,26]. Using in situ FT-IR spectroscopy, the gas phase products (carbon dioxide and carbon monoxide) and the principal intermediate involved in the catalytic conversion of methane, e.g. methoxy, dioxymethylene and adsorbed formaldehyde species, were identified. Based on these observations a reaction model was proposed, and then kinetic studies were carried out using a catalyst with a Mo/Fe ratio of 1.7. As previously described, this is the most complete and reliable kinetic model for the heterogeneous catalytic partial oxidation of methane reported in modern literature, and it was used in the present study. The kinetic parameters of the elementary reactions and the mechanism for catalytic partial oxidation of methanol on ferric molybdate proposed by Fuangfoo are shown in Table 2.

Table 2
Reaction parameters for catalytic partial oxidation of methanol

Reaction	A (min^{-1})	E (kJ/mol)
$CH_4 + MO \rightarrow MOCH_3 + \frac{1}{2}H_2$	9.40E+16	255.9
$MOCH_3 \rightarrow MOCH_2 + \frac{1}{2}H_2$	2.20E+00	44.8
$MOCH_3 + MO \rightarrow MOCH_2OM + \frac{1}{2}H_2$	7.40E+08	146.9
$MOCH_2 + MO \rightarrow MOCHOM + \frac{1}{2}H_2$	4.60E+08	133.3
$MOCH_2OM \rightarrow MOCHOM + \frac{1}{2}H_2$	5.70E−02	9.5
$MOCHOM \rightarrow M + MOH + CO$	3.20E−01	17.9
$MOCH_2OM \rightarrow 2M + CO_2 + H_2$	3.20E−04	1.3
$MOCH_3 + \frac{1}{2}H_2 \rightarrow M + CH_3OH$	4.10E−04	99.5
$MOCH_2OM \rightarrow 2M + CO_2 + H_2$	3.00E−04	84.8

M and MO represent the reduced and oxidized catalytic sites, respectively.

2.5. *Transport and thermodynamic properties*

A fundamental part of the model is the set of constitutive equations to determine thermodynamic and transport properties of the mixture (density, heat capacity, enthalpy, thermal conductivity, viscosity and diffusion coefficients).

Viscosity and conductivity of the mixture were determined using Chung method [45–47]:

$$\eta = \eta^* \frac{36.344(MT_s)^{1/2}}{T_c^{2/3}} \tag{2}$$

$$\lambda = \frac{31.2\eta^0 \Psi}{M'}(G_2^{-1} + B_6 y) + qB_7 y^2 T_r^{1/2} \tag{3}$$

Parameters of the previous equations are calculated using expressions for pure components and mixture rules given by Chung et al. [45–47]. Diffusion coefficients of the mixture were estimated using the method of Fuller et al. [45,48].

$$D_{ij} = \frac{0.00143T^{1.75}}{PM_{ij}^{1/2}\left[\left(\sum v\right)_i^{1/3} + \left(\sum v\right)_j^{1/3}\right]^2} \tag{4}$$

Diffusion volumes are calculated from atomic contributions. Diffusion coefficients for each component in the mixture are estimated using the law of Blanc, reported in Poling et al. [45]:

$$D_{im} = \left(\sum_{\substack{j=1 \\ j \neq i}}^{n} \frac{x_j}{D_{im}} \right)^{-1} \tag{5}$$

Gas phase densities and enthalpies were estimated using the cubic Peng–Robinson equation [45]:

$$P = \frac{RT}{V-b} - \frac{a[1+(0.37464+1.54226\omega - 0.26996\omega^2)(1-T_{\mathrm{r}}^{1/2})]^2}{(V^2+2bV-b^2)} \qquad (6)$$

2.6. Adsorbent model

Starting from the characteristics and parameters found for the selected adsorbent, the adsorption processes of the gas mixture components on this material were modeled. Adsorption parameters values are determined experimentally for the selected adsorbents. The models used for the selected adsorbents are:

Langmuir adsorption model

$$C = C_{\mathrm{H}}\left[\frac{bP}{1+bP}\right] \qquad (7)$$

Combined Henry–Langmuir adsorption model

$$C = C_{\mathrm{H}}\left[\frac{bP}{1+bP}\right] + k_{\mathrm{D}}P \qquad (8)$$

2.7. Balance equations

The studied system has three phases, one gas phase and two solid phases. The equations used for modeling the mass, energy and momentum transfer processes are the balance equations adapted for gas-particle systems [49–51]. These equations have usually been applied to simple cases with one solid phase, and in some cases even the reaction in a single phase has been considered. In the present case, the equations were applied to a system conformed by one gas phase and two solid phases (adsorbent and catalyst), taking into account the chemical reactions in two phases: homogeneous chemical reaction in the gas phase and catalytic chemical reaction to the interior of a solid phase, as well as the chemical adsorption on the second solid phase.

Gas phase continuity equation:

$$\frac{\partial}{\partial t}(\rho_{\mathrm{g}}\varepsilon_{\mathrm{g}}) + \nabla\cdot(\rho_{\mathrm{g}}\varepsilon_{\mathrm{g}}\vec{v}_{\mathrm{g}}) = \sum R_{gn} \qquad (9)$$

Solid phases continuity equation:

$$\frac{\partial}{\partial t}(\rho_{\mathrm{s}}\varepsilon_{\mathrm{s}}) + \nabla\cdot(\rho_{\mathrm{s}}\varepsilon_{\mathrm{s}}\vec{v}_{\mathrm{s}}) = \sum R_{sn} \qquad (10)$$

Gas phase energy balance:

$$\rho_{\mathrm{g}}\varepsilon_{\mathrm{g}}C_{\mathrm{p_g}}\left(\frac{\partial T_{\mathrm{g}}}{\partial t} + \vec{v}_{\mathrm{g}}\cdot\nabla T_{\mathrm{g}}\right) = \nabla\vec{q}_{\mathrm{g}} + \gamma_{\mathrm{gs}}(T_{\mathrm{s}}-T_{\mathrm{g}}) - \sum_{i=1}^{nrg} R_i\Delta H_{\mathrm{rg}} + H_{\mathrm{wall}}(T_{\mathrm{wall}}-T_{\mathrm{g}}) \qquad (11)$$

Solid phases energy balance:

$$\rho_{\mathrm{s}}\varepsilon_{\mathrm{s}}C_{\mathrm{p}}\left(\frac{\partial T_{\mathrm{s}}}{\partial t} + \vec{v}_{\mathrm{s}}\cdot\nabla T_{\mathrm{s}}\right) = \nabla\vec{q}_{\mathrm{s}} + \gamma_{\mathrm{gs}}(T_{\mathrm{s}}-T_{\mathrm{g}}) - \sum_{j=1}^{nrs} R_i\Delta H_{\mathrm{rs}} \qquad (12)$$

Gas phase momentum balance:

$$\frac{\partial}{\partial t}(\rho_{\mathrm{g}}\varepsilon_{\mathrm{g}}\vec{v}_{\mathrm{g}}) + \nabla\cdot(\rho_{\mathrm{g}}\varepsilon_{\mathrm{g}}\vec{v}_{\mathrm{g}}\vec{v}_{\mathrm{g}}) = -\nabla P_{\mathrm{g}} + \nabla\cdot\bar{\bar{\tau}}_{\mathrm{g}} + \rho_{\mathrm{g}}\varepsilon_{\mathrm{g}}\vec{g} + F_{\mathrm{gs}}(\vec{v}_{\mathrm{s}}-\vec{v}_{\mathrm{g}}) - R_{\mathrm{os}}(\xi_{\mathrm{os}}\vec{v}_{\mathrm{s}} + \bar{\xi}_{\mathrm{os}}\vec{v}_{\mathrm{g}}) \qquad (13)$$

Solid phases momentum balance:

$$\frac{\partial}{\partial t}(\rho_{\mathrm{s}}\varepsilon_{\mathrm{s}}\vec{v}_{\mathrm{s}}) + \nabla\cdot(\rho_{\mathrm{s}}\varepsilon_{\mathrm{s}}\vec{v}_{\mathrm{s}}\vec{v}_{\mathrm{s}}) = -\nabla S_{\mathrm{s}} + \rho_{\mathrm{s}}\varepsilon_{\mathrm{s}}\vec{g} - F_{\mathrm{gs}}(\vec{v}_{\mathrm{s}}-\vec{v}_{\mathrm{g}}) - R_{\mathrm{os}}(\xi_{\mathrm{os}}\vec{v}_{\mathrm{s}} + \bar{\xi}_{\mathrm{os}}\vec{v}_{\mathrm{g}}) \qquad (14)$$

Gas phase molar balance:

$$\frac{\partial}{\partial t}(\rho_{\mathrm{g}}\varepsilon_{\mathrm{g}}X_{gn}) + \nabla\cdot(\rho_{\mathrm{g}}\varepsilon_{\mathrm{g}}X_{gn}\vec{v}_{\mathrm{g}}) = \nabla\cdot D_{gn}\nabla\cdot X_{gn} + R_{gn} \qquad (15)$$

Solid phases molar balance:

$$\frac{\partial}{\partial t}(\rho_{\mathrm{s}}\varepsilon_{\mathrm{s}}X_{sn}) + \nabla\cdot(\rho_{\mathrm{s}}\varepsilon_{\mathrm{s}}X_{sn}\vec{v}_{\mathrm{s}}) = R_{sn} \qquad (16)$$

An expression to estimate the drag in the solid phases and a turbulence model for the system, such as the κ–ε model are needed. Another necessary expression is the conservation of granular energy in the solid phases:

$$\frac{3}{2}\left[\frac{\partial}{\partial t}(\rho_{\mathrm{s}}\varepsilon_{\mathrm{s}}\Theta_{\mathrm{s}}) + \nabla\cdot(\rho_{\mathrm{s}}\varepsilon_{\mathrm{s}}\Theta_{\mathrm{s}})\vec{v}_{\mathrm{s}}\right] = \bar{\bar{S}}_{\mathrm{s}} : \nabla\vec{v}_{\mathrm{s}} - \nabla\cdot\vec{q}_{\Theta_{\mathrm{s}}} - \gamma_{\Theta_{\mathrm{s}}} + \phi_{\Theta_{\mathrm{s}}} \qquad (17)$$

The obtained model after simplification for stationary state is a system of partial differential equations. The solution of this system of equations was carried out using a Fortran program and the NAG mathematical libraries [52].

3. Results

The obtained system was first analyzed from the reactor design point of view. A search for the optimal characteristics, such as height and diameter of the equipment, diameter of the catalyst grains and of the absorbent was made. From the mathematical point of view, the problem is the restricted optimization of a system of partial differential equations. This problem was solved with the use of the Fortran language and the Numerical Algorithms Group (NAG) mathematical libraries [52]. The best configuration obtained for the design of the reactor is the one presented in Table 3.

Table 3
Best configuration for the design of the GSS reactor

Design variables	Value
Catalyst column height	5.5E−1 m
Column diameter	9.25E−2 m
Catalyst particle diameter	7.85E−3 m
Adsorbent particle diameter	1.35E−5 m

Table 4
Best configuration for the operation variables of the GSS reactor

Operational variable	Value
Gases inlet pressure (bottom of the reactor) (Pa)	8.56e6
Gases inlet temperature (bottom of the reactor) (K)	452.3
Gases exit temperature (top of the reactor) (K)	514.0
Adsorbent inlet temperature (top of the reactor) (K)	355.4
Adsorbent exit temperature (bottom of the reactor) (K)	511.0
Feed ratio O_2/CH_4	1/8.5
Unconverted CH_4 (%)	89.81
Yield	
CH_3OH (%)	6.47
CHO (%)	2.22
CO_2 (%)	1.37
CO (%)	0.14

In a following step the optimization of the operation variables, such as pressure, temperature and feed ratio was established. The values of the operation variables with the best-obtained configuration are shown in Table 4.

For comparison purposes, a simulation of a conventional fixed bed (FB) reactor with the same dimensions and under the same operation conditions was carried out. The calculated conversion of methane to methanol was of 1.38%. This is more than four times smaller than the one calculated for the GSS reactor (Fig. 2).

In Fig. 3, the longitudinal average temperature profile for the gases and solid adsorbent in the best reactor configuration is shown. The areas of the reactor at high temperatures are favorable for formaldehyde and carbon oxides reactions. Similarly, high temperatures are not favorable for methanol adsorption in detriment of its conversion and therefore, increasing the formation of formaldehyde.

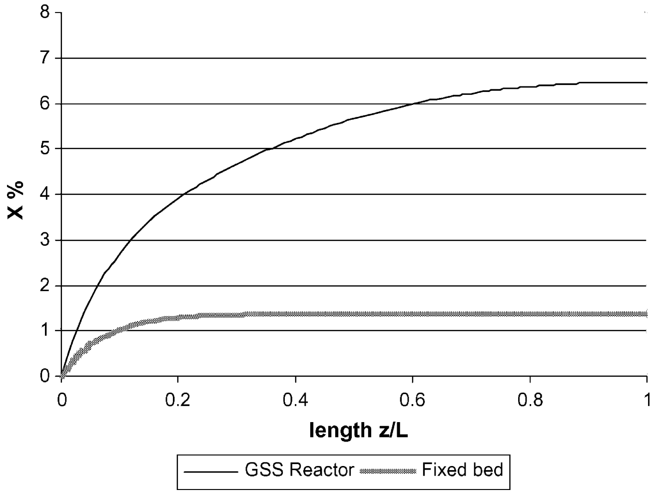

Fig. 2. Average conversion of methane to methanol in a gas–solid–solid reactor and in a conventional fixed bed reactor as a function of the reactor length.

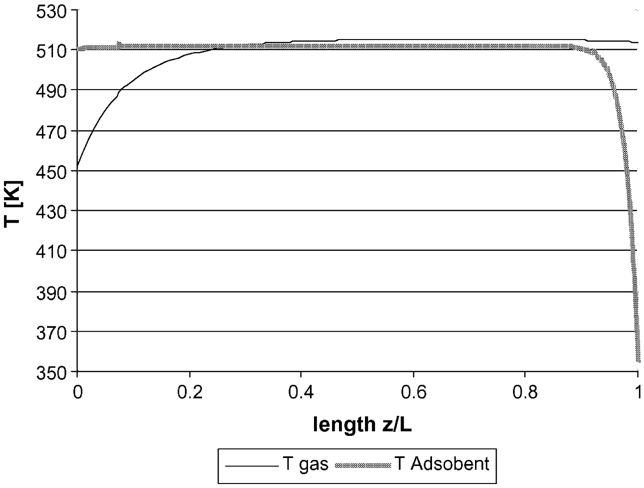

Fig. 3. Longitudinal gas–solid–solid reactor temperature profile.

In spite of the high conversion levels in comparison with a conventional FB reactor, the reached levels could not be applied in an industrial reactor. Therefore, an improvement in the GSS system implementing a continuous lateral supply of oxygen was proposed, as shown in Fig. 4. In this new configuration of the reactor, the oxygen is supplied laterally along of the reactor, so that the amount exactly required to maximize the selectivity to

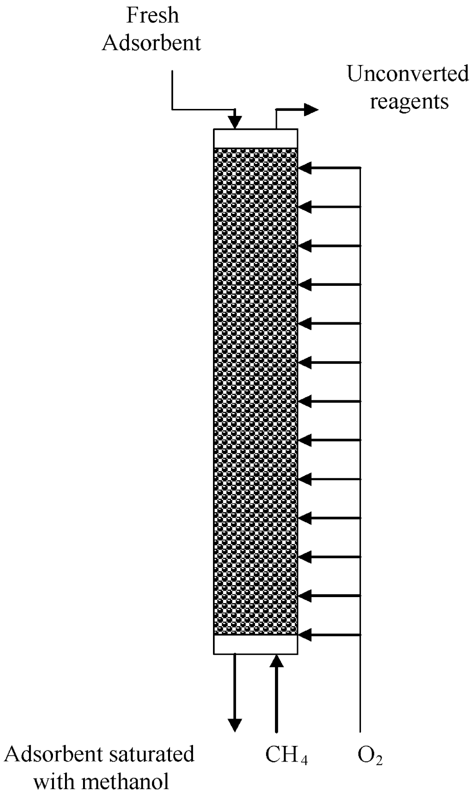

Fig. 4. Scheme of the gas–solid–solid reactor with continuous oxygen supply.

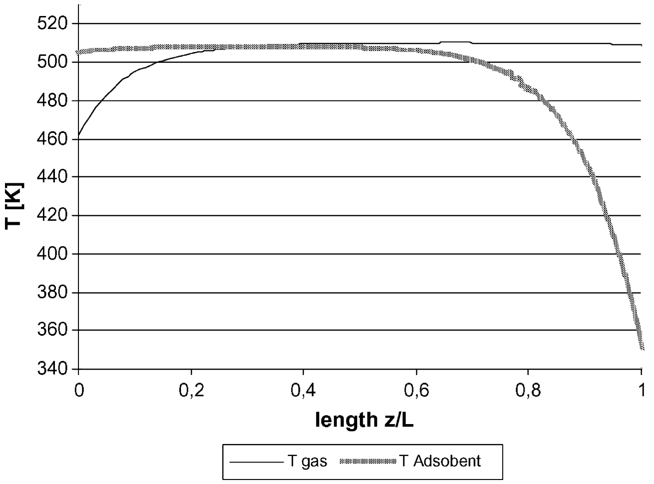

Fig. 5. Longitudinal reactor temperature profile of the GSS reactor with lateral supply of oxygen.

methanol is supplied. In the practice this could be obtained with multiple lateral inlets to the reactor, each one of them with the diameter exactly calculated to give the desired flow. An additional effect achieved with the new design is the reduction in the gas temperature with cold oxygen. This factor can help to maintain a better profile of temperature that could favor the methanol adsorption.

Using the values of column diameter, catalyst diameter and adsorbent particle diameter initially calculated an optimization of the GSS reactor including the lateral supply of oxygen was done. The values of the operational variables for the improved GSS reactor are shown in Table 4. In Fig. 5, the average temperature profile for the gases and solid adsorbent for the best reactor configuration with continuous oxygen supply is presented (Table 5).

The increase in the methanol conversion was because the controlled lateral supply of oxygen led to an increased methanol selectivity by avoiding the formation of other oxygenated derivates, such as formaldehyde and carbon oxides. Additionally, the oxygen lateral feeding acts as a coolant leading to lower adsorbent exit temperatures, and achieving in this way a better product adsorption.

Table 5
Best configuration for the GSS reactor with lateral supply of oxygen

Operational variable	Value
Gases inlet pressure (bottom of the reactor) (Pa)	8.79e6
Gases inlet temperature (bottom of the reactor) (K)	461.7
Gases exit temperature (top of the reactor) (K)	508.8
Adsorbent inlet temperature (top of the reactor) (K)	355.4
Adsorbent exit temperature (bottom of the reactor) (K)	505.6
Feed ratio O_2/CH_4	1/4.56
Unconverted CH_4 (%)	89.81
Yield	
CH_3OH (%)	17.62
CHO (%)	1.54
CO_2 (%)	1.01
CO (%)	0.33

4. Conclusions and recommendations

A new and promising alternative for methanol synthesis from methane was proposed using a gas–solid–solid reactor for the intensification of the reaction by means of a selective adsorption with a silica–alumina. The proposed methodology was used to obtain the mathematical model of a gas–solid–solid reactor for the methane partial oxidation at relatively low temperatures. The calculations showed that the use of a selective adsorbent improved the results in comparison with a conventional FB reactor, increasing more than 12 times the methanol conversion.

The advantages of this reactor design open a great alternative for the intensification of industrial processes that present as common characteristic low conversions as it is the case for the direct conversion of methane to methanol.

It is evident that the increase in the adsorbent temperature is a limiting factor for the reached conversion level. Although the calculated conversions were considerably superior to those achieved in a catalytic fixed bed reactor, a better behavior could be possible by controlling the adsorbent heating.

The limitations in the conversion due to adsorbent heating, therefore present an opportunity for the development of improvements in the proposed process. An alternative that could improve the gas–solid–solid reactor with continuous oxygen supply is an additional low temperature oxygen supply, as is shown in the scheme of Fig. 6. In this configuration of the reactor, the oxygen is supplied laterally along of the reactor from two sources, so that the amount exactly required to optimize the temperature in the adsorbent is supplied. This new design can help to maintain a better profile of temperature and therefore better conversions.

Another alternative design is a multiple bed reactor with heat exchange between beds, as shown in the scheme of Fig. 7.

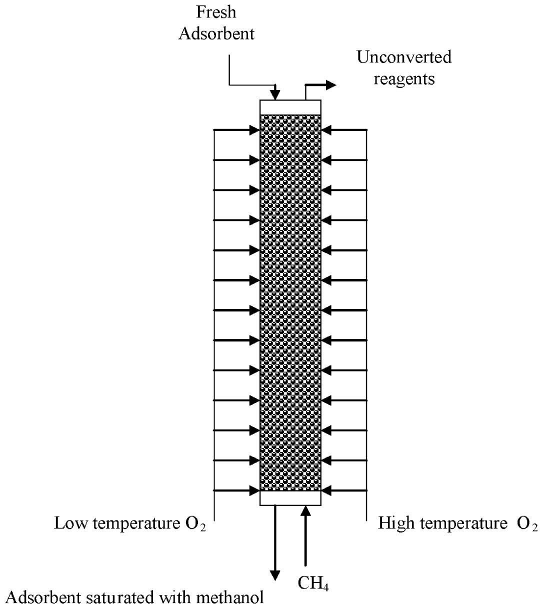

Fig. 6. Scheme of the gas–solid–solid reactor with continuous supply of high and low temperature oxygen.

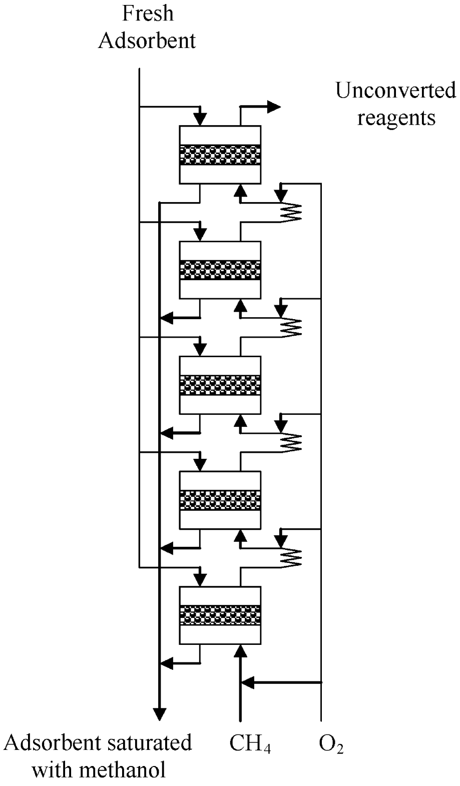

Fig. 7. Scheme of a multiple beds gas–solid–solid reactor.

This reactor would allow maintaining lower temperatures in the adsorbent and higher levels of adsorption and therefore larger conversions, because the temperature excess is removed after each stage.

Acknowledgments

We thank the financial support for this investigation by the DIF of physical chemical sciences of the Industrial University of Santander (UIS) through project 5402, the laboratory of optimization, design and advanced control of processes of the State University of Campinas (UNICAMP), and COLCIENCIAS-ICETEX through the Program of National Doctorates.

References

[1] W. Tsang, R.F. Hampson, Chemical kinetic dates base for combustion chemistry. Part 1. Methane and related compounds, J. Phys. Chem. Ref. Data 15 (1986) 1087–1279.

[2] W. Tsang, Chemical kinetic data base for combustion chemistry. Part 2. Methanol, J. Phys. Chem. Ref. Data 16 (1987) 471–508.

[3] P.S. Yarlagadda, et al., Direct conversion of methane to methanol in a flow reactor, Ind. Eng. Chem. Res. 27 (1988) 252–256.

[4] P.S. Casey, T. McAllister, K. Foger, Selective oxidation of methane to methanol at high pressures, Ind. Eng. Chem. Res. 33 (1994) 1120–1126.

[5] V.I. Vedeneev, et al., The role of initiation in oxidative coupling of methane, Appl. Catal. A 127 (1995) 51–63.

[6] O. Liu, et al., Improved methanol yield from methane oxidation in a non-isothermal reactor, Fuel 75 (1996) 1748–1754.

[7] Y. Teng, et al., Methanol formation from methane partial oxidation in CH_4-O_2–NO gaseous phase at atmospheric pressure, Appl. Catal. A 190 (2000) 283–289.

[8] Q. Zhang, Comparatively high yield methanol production from gas phase partial oxidation of methane, Appl. Catal. A 224 (2002) 201–207.

[9] B. Mhadeshwar, D.G. Vlachos, Hierarchical multiscale mechanism development for methane partial oxidation and reforming and for thermal decomposition of oxygenates on Rh, J. Phys. Chem. B 109 (2005) 16819–16835.

[10] C.K. Westbrook, F.L. Dryer, Chemical kinetic modeling of hydrocarbon combustion, Prog. Energy Combust. Sci. 10 (1984) 1–57.

[11] R.A. Strehlow, Combustion Fundamentals, McGraw-Hill, New York, USA, 1984.

[12] W.J. Pitz, C.K. Westbrook, Chemical kinetics of the high pressure oxidation of *n*-butane and its relation to engine knock, Combust. Flame 63 (1986) 113–133.

[13] P. Dagaut, et al., Kinetic modeling of propane oxidation, Combust. Sci. Technol. 56 (1987) 23–63.

[14] W. Bartok, A.F. Sarofim, Fossil Combustion, a Source Book, Wiley, USA, 1991.

[15] K. Okazaki, et al., Direct conversion of methane to methanol by a pulsed silent discharge, in: 29th Symp. Heat Transfer, Osaka, Japan, 1992.

[16] M. Bistol, et al., Kinetic model for methane oxidative coupling reactors, Chem. Eng. Sci. 47 (1992) 2647–2652.

[17] B.S. Rajnikanth, et al., Application of pulsed discharge plasma for methanol synthesis, in: Conf. Rec. IEEE/IAS Annual Meeting, 1995, pp. 1459–1462.

[18] T. Kodama, et al., High-temperature reactions on metal oxides of CH_4 with H_2O to from C_2H_4, CO and H_2, Energy Int. J. 22 (1997) 859–866.

[19] J. Warnatz, U. Mass, R.W. Dibble, Combustion, second ed., Springer, New York, USA, 1999.

[20] A.S. Feitelberg, S.M. Corream, The role of carbon monoxide in NO_2 plume formation, J. Eng. Gas Turbines Power (Trans. ASME) 122 (2000) 287–292.

[21] S.S. Verma, To study the direct transformation of methane into methanol in the lower temperature range, Energy Convers. Manage. 43 (2002) 1999–2008.

[22] M.D. Amiridis, et al., Simulation of methane partial oxidation over silica-supported MoO_3 and V_2O_5, AIChE J. 37 (1991) 87–97.

[23] S. Chellappa, D.S. Viswanath, Partial oxidation of methane using ferric molybdate catalyst, Ind. Eng. Chem. Res. 34 (1995) 1933–1940.

[24] S. Chellappa, Methane conversion to methanol-homogeneous and catalytic studies, Ph.D. Thesis, UMI, USA, 1997.

[25] N.D. Spencer, Partial oxidation of methane to formaldehyde by means of molecular oxygen, J. Catal. 109 (1988) 187–197.

[26] N.D. Spencer, C.J. Pereira, Partial oxidation of CH_4 to HCHO over MoO_3-SiO_2 catalyst: a kinetic study, AIChE J. 33 (1987) 1808–1812.

[27] P. Paredes Olivera, E.M. Patrito, H. Sellers, Direct synthesis of methanol over metallic catalysts, Surf. Sci. 327 (1995) 330–357.

[28] K. Otsuka, Y. Wang, Direct conversion of methane into oxygenates, Appl. Catal. A 222 (2001) 145–161.

[29] P.P. Knops-Gerrits, W.A. Goddard III, Methane partial oxidation in iron zeolites: theory versus experiment, J. Mol. Catal. A: Chem. 166 (2001) 135–145.

[30] T. Takemoto, et al., The optimization of methanol yield in direct selective oxidation of methane with O_2 and NO in the presence of Cu-ZnO/Al2O3, J. Mol. Catal. A Chem. 179 (2002) 279–286.

[31] Q. Zhang, Controlled partial oxidation of methane to methanol/formaldehyde over Mo-V-Cr-Bi-Si oxide catalysts, Fuel Process. Technol. 81 (2002) 1599–1603.

[32] X. Wang, et al., Mcm-41-supported iron phosphate catalyst for partial oxidation of methane to oxygenates with oxygen and nitrous oxide, J. Catal. 217 (2003) 457–4673.

[33] S. Fuangfoo, FT-IR Studies on partial oxidation of methane over ferric molybdate catalysts, Ph.D. Thesis, UMI, USA, 1997.

[34] K.R. Westerterpt, M. Kuczynski, A model for a countercurrent gas-solid-solid trickle flow reactor for equilibrium reactions. The methanol synthesis, Chem. Eng. Sci. 42 (1987) 1871–1885.

[35] K.R. Westerterp, M. Kuczynski, C.H.M. Kamphuis, Synthesis of methanol in a reactor system with interstage product removal, Ind. Eng. Chem. Res. 28 (1989) 763–771.

[36] K.R. Westerterp, Multifunctional reactors, Chem. Eng. Sci. 47 (1992) 2195–2206.

[37] J.H.A. Kie, W. Prins, W.P.M. Van Swaaij, Mass transfer between gas and particles in a gas-solid trickle flow reactor, Chem. Eng. Sci. 48 (1993) 117–125.

[38] Z.J. Predojevic, D.L.J. Petrovic, A.P. Dudukovic, Modeling and predictions of solids dynamic holdup in gas-flowing solids-fixed bed contactors, Ind. Eng. Chem. Res. 40 (2001) 6039–6043.

[39] L.V. Barysheva, et al., Motion of particles through the fixed bed in a gas–solid–solid downflow reactor, Chem. Eng. J. 91 (2003) 219–225.

[40] P. Dudukovic, N.M. Nikacevic, Z.V. Kuzeljevic, Modeling and predictions of solids dynamic holdup in gas-flowing solids-fixed bed contactors, Ind. Eng. Chem. Res. 43 (2004) 7445–7448.

[41] N.M. Nikacevic, A.P. Dudukovic, Solids residence time distribution in gas-flowing solids-fixed bed contactors, Ind. Eng. Chem. Res. 44 (2005) 6509–6517.

[42] V. Kafarov, Flexible laboratory system for investigation of catalytic processes, Per. Pol. Chem. Eng. 38 (1994) 93–97.

[43] V. Kafarov, C.G. Dallos, L. Acevedo, Dynamic experimentation for identification of porous structure of coal based activated carbons, in: Proceeding of Sixth Conference on Environment and Mineral Processing, 2002, pp. 307–311.

[44] V. Kafarov, New method for research of catalytic processes, COLCIENCIAS Project, Códe: 1102-06-246-96, 2000.

[45] E. Poling, J.M. Prausnitz, J.P. O'Conell, The Properties of Gases and Liquids, The McGraw Hill Companies, USA, 2001.

[46] T.H. Chung, et al., Applications of kinetic gas theories and multiparameter correlation for prediction of dilute gas viscosity and thermal conductivity, Ind. Eng. Chem. Fundam. 23 (1984) 8–13.

[47] T.H. Chung, et al., Generalized multiparameter correlation for nonpolar and polar fluid transport properties, Ind. Eng. Chem. Res. 27 (1988) 671–679.

[48] E.N. Fuller, P.D. Schettler, J.C. Giddings, A new method for prediction coefficients of binary gas-phase diffusion, Ind. Eng. Chem. 58 (1966) 18–27.

[49] M. Syamlal, MFIX Documentation Numerical Technique, U.S. Department of Energy, 1998.

[50] M. Wallace, Simulation of cohesive particle flows in granular and gas–solid systems, Ph. D. Thesis, University of Colorado, USA, 1998.

[51] D. Boyalakuntla, Simulation of granular and gas-solid flows using discrete element method, Ph.D. Thesis, CMU, USA, 2003.

[52] NAG, The Numerical Algorithms Group Ltd., UK, 2006 (website: www.nag.co.uk).